

Solitons in hydrogen-bonded chains

D. Hochstrasser and H. Büttner

Physikalisches Institut, Universität Bayreuth, D-8580 Bayreuth, Federal Republic of Germany

H. Desfontaines and M. Peyrard

Laboratoire d'Optique du Réseau Cristallin, Université de Dijon, F-21100 Dijon, France

(Received 18 April 1988)

A one-dimensional model for hydrogen-bonded chains is investigated by including the dynamical degrees of freedom of the oxygens and thus generalizing the original Antonchenko-Davydov-Zolotaryuk model. Analytical solutions are derived within a continuum approximation up to second order so that rather narrow solutions could be derived accurately enough. Numerical simulations with a set of parameters derived from infrared spectra show stable low- and high-speed solutions separated by a forbidden gap. There exists also an intermediate velocity range where the initial pulse is unstable in the sense that it is transformed to a high-speed solution with the same energy. Discreteness effects are discussed.

I. INTRODUCTION

Since the basic work of Antonchenko *et al.*¹ and Zolotaryuk *et al.*² there has been great interest in the soliton dynamics in one-dimensional hydrogen-bonded systems. These models seem to be an effective description of the proton mobility in hydrogen-bonded chains, and therefore may also play a role in interpreting certain biological processes in such systems.³ Since the work of Bernal and Fowler⁴ the hydrogen bonds have been described by some kind of double-minimum potential. The high proton mobility is given by a hopping contribution for the protons from one of the minima into the other. The particular mechanism, however, is not yet understood in detail. On the other hand, the soliton picture for transport in biological macromolecules has been discussed intensively in the literature and seems to be one possible mechanism in some of these processes.⁵⁻⁷

Besides the model by Antonchenko *et al.* which describes the hydrogen bond as a ϕ^4 potential, there has been another model where the dynamics of the hydrogen is given within the pseudospin formalism.⁸⁻¹¹ In both cases the hydrogens alternate within the chain with oxygen ions. This simple ice structure with harmonic oxygen-oxygen and hydrogen-hydrogen coupling, a nonlinear hydrogen on-site potential, and a nonlinear hydrogen-oxygen interaction leads to two coupled nonlinear difference equations. The origin of the nonlinear on-site potential for the hydrogen is not further described here, but one assumes that the detailed interaction mechanism may result in such a potential. In the same sense the oxygen-hydrogen interaction is regarded as an effective term. Since one assumes an on-site potential, one expects as excitations a topological solitary wave for the hydrogens and a nontopological excitation for the oxygens. Antonchenko *et al.* found in their model analytic solutions in the continuum approximation only for a certain solitary wave velocity. Further work on this model^{12,13} has established existence of solutions in a far

greater range of velocities and has studied the stability of these solutions. There are also modifications of the original model by Zolotaryuk,¹⁴ where for a wide class of general interactions two velocity regions of solutions were found.

The original model of Antonchenko *et al.*¹ did not include all degrees of freedom of the oxygens because a single variable describing their relative motion was used for a pair of oxygen atoms. The model that we treat in this paper includes all degrees of freedom for the oxygens. A similar model was previously considered in a continuum approximation by Zolotaryuk *et al.*;² however, we start here from a discrete model because we found that, when reasonable parameter values are considered, the solutions are rather narrow. Although we have to use a continuum approximation to derive an analytical solution, we include higher-order terms which are necessary to provide a correct description of the lattice effects. Section II presents the model. In Sec. III we discuss analytic solutions for the continuum model in the whole range of velocities. In Sec. IV we discuss the various parameters and give the energies of the solutions as a function of these parameters. In Sec. V we discuss the stability of the linearized lattice, while in Sec. VI the numerical investigations are discussed in some detail.

II. THE MODEL HAMILTONIAN

Our model similar to the one by Antonchenko *et al.*¹ consists of a diatomic chain of protons and oxygen atoms (Fig. 1). The total Hamiltonian consists of three parts. The proton part is given by

$$H_p = \sum_n \left[\frac{m}{2} [\dot{u}_n^2 + \omega_1^2 (u_{n+1} - u_n)^2] + \varepsilon V(u_n) \right], \quad (2.1)$$

with the onsite potential of strength ε :

$$V(u_n) = [1 - (u_n/b)^2]^2. \quad (2.2)$$

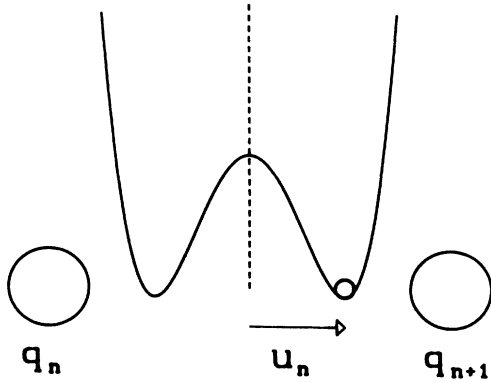


FIG. 1. Hydrogen bond. The proton in the Φ^4 potential is drawn. The large circles correspond to the oxygen sublattice.

The proton coordinate u_n is the displacement of the hydrogen from the middle of the bond as it is shown in Fig. 1.

The oxygen Hamiltonian is written as

$$H_O = \sum_n \frac{M}{2} [\dot{q}_n^2 + \Omega_1^2 (q_{n+1} - q_n)^2], \quad (2.3)$$

where q_n describes the displacement from the equilibrium position. In the original model of Antonchenko *et al.* only optical vibrations were considered, whereas in our model acoustic vibrations are included.

The interaction is as in Antonchenko's model:

$$H_i = \chi \sum_n (q_{n+1} - q_n)(u_n^2 - b^2). \quad (2.4)$$

The physical content of this interaction is the lowering of the double potential barrier due to the oxygen displacements. We note here that it is also possible to get analytic solutions with a slight generalization of H_i by changing the $u_n^2 - b^2$ term to a general function $W(u_n)$ (cf. Zolotaryuk¹⁴).

The parameters in our model are the harmonic lattice frequencies ω_1, Ω_1 , the coupling constant χ , the barrier energy ε , and the width b of the potential. The actual values of these parameters will be discussed later. The classical equations of motions are written in a dimensionless form with the following notation:

$$\begin{aligned} \varphi_n &= u_n/b, \quad \psi_n = q_n/q, \quad \tau = t/t_1, \\ q &= \chi b^2 / (2M\Omega_1^2), \quad t_1 = 1/\omega_1, \quad \alpha = \chi q / (m\omega_1^2), \\ \beta &= \varepsilon / (mb^2\omega_1^2), \quad \gamma^2 = \Omega_1^2 / \omega_1^2. \end{aligned} \quad (2.5)$$

With these abbreviations one finds

$$\begin{aligned} -\frac{d^2\varphi_n}{dt^2} + (\varphi_{n+1} + \varphi_{n-1} - 2\varphi_n) - \frac{\beta\partial V}{\partial\varphi_n} \\ + 2\alpha\varphi_n(\psi_{n+1} - \psi_n) = 0, \end{aligned} \quad (2.6)$$

$$\begin{aligned} -\frac{1}{\gamma^2} \frac{d^2\psi_n}{dt^2} + (\psi_{n+1} + \psi_{n-1} - 2\psi_n) + 2(\varphi_{n-1}^2 - \varphi_n^2) = 0. \end{aligned} \quad (2.7)$$

We note here that we know of no solution for the discrete lattice equations, and therefore we try to find consistent equations in the continuum approximation. This approximation has to be done up to a certain order in the lattice parameter a . We will approximate the Hamiltonian up to second order in this parameter (the first-order approximation in the interaction part corresponds to a Lagrange density discussed by Zolotaryuk *et al.*²).

III. SOLITARY SOLUTIONS IN THE CONTINUUM APPROXIMATION

For solutions which change slowly compared to the lattice spacing, one can use the continuum approximation. The resulting equations of motion are as follows (where we have scaled the lattice constant a to 1):

$$\varphi_{yy} - \varphi_{\tau\tau} - \beta \frac{\partial V}{\partial\varphi} + \alpha\varphi(2\psi_y + \psi_{yy}) = 0, \quad (3.1)$$

$$\psi_{yy} - \psi_{\tau\tau} / \gamma^2 - 2(\varphi^2)_y + (\varphi^2)_{yy} = 0. \quad (3.2)$$

From the special form of the interaction Hamiltonian it follows that the interaction between the two sublattices is quadratic in these expressions. Since we are only interested in running wave solutions with velocity c the partial differential equations can be transformed to ordinary differential equations for a single variable $z = y - c\tau$. From the equations of motion one then can do one integration in Eq. (3.2) and find

$$\frac{d\psi}{dz} = \psi' = [2(\varphi^2 - 1) - (\varphi^2)'] / (1 - c^2/\gamma^2). \quad (3.3)$$

Here we have used the following boundary conditions for solitary solutions, which are appropriate for a solitary wave:

$$\begin{aligned} \lim_{|z| \rightarrow \infty} |\varphi(z)| &= 1, \\ \lim_{|z| \rightarrow \infty} \psi'(z) &= 0, \end{aligned}$$

and all derivatives are vanishing at large z . Now the two coupled ordinary differential equations are separated and the remaining equation in $\varphi(z)$ can be integrated at once with the result

$$\frac{d\varphi}{dz} = \varphi' = \pm (1 - \varphi^2) / \left[\frac{B - \varphi^2}{A} \right]^{1/2}, \quad (3.4)$$

where we have used the following parameter functions:

$$A = \beta(1 - c^2/\gamma^2)/\alpha - 1, \quad B = (1 - c^2)(1 - c^2/\gamma^2)/(2\alpha). \quad (3.5)$$

Depending on these parameters A and B two different kinktype solutions are found: For $A > 0$ and $B > 1$ one finds

$$\begin{aligned} \eta z = \pm \left[\frac{(\kappa^2 - 1)^{1/2}}{2} \ln \left| \frac{(\kappa^2 - \varphi^2)^{1/2} + (\kappa^2 - 1)^{1/2} \varphi}{(\kappa^2 - \varphi^2)^{1/2} - (\kappa^2 - 1)^{1/2} \varphi} \right| \right. \\ \left. + \arcsin(\varphi/\kappa) \right]. \end{aligned} \quad (3.6)$$

For $A < 0$ and $B < 0$ we have instead

$$\eta z = \pm \left[\frac{(\kappa^2 + 1)^{1/2}}{2} \ln \left| \frac{(\kappa^2 + \varphi^2)^{1/2} + (\kappa^2 + 1)^{1/2} \varphi}{(\kappa^2 + \varphi^2)^{1/2} - (\kappa^2 + 1)^{1/2} \varphi} \right| - \ln \frac{(\kappa^2 + \varphi^2)^{1/2} \pm \varphi}{\kappa} \right], \quad (3.7)$$

where we used the following abbreviations: $\kappa^2 = |B|$, $\eta^2 = |A|$. These somewhat seemingly complicated functions result in kinklike structures for $\varphi(z)$.

IV. DISCUSSION OF PARAMETERS AND ENERGIES

The velocity ranges of the two kinklike solutions [Eqs. (3.6) and (3.7)] follow from the definitions of the parameters A and B in Eq. (3.5). If we introduce the additional abbreviations

$$c_1^2 = \gamma^2(1 - \alpha/\beta), \quad (4.1)$$

$$2c_2^2 = 1 + \gamma^2 - [(1 - \gamma^2)^2 + 8\gamma^2\alpha]^{1/2},$$

we can distinguish between mainly two different cases.

(a) In this case the speed of sound in the oxygen sublattice is smaller than the corresponding velocity in the hydrogen sublattice. For our parameters this means $\gamma^2 < 1$ and

$$A > 0, B > 1$$

$$\text{for } 0 < c^2 < \min(c_1^2, c_2^2) \text{ with } \alpha < 0.5, \alpha/\beta < 1$$

or

$$A < 0, B < 0 \text{ for } \gamma^2 < c^2 < 1 \text{ with } \alpha, \beta > 0.$$

(b) In the reverse case with the hydrogen speed of sound less than the oxygen speed of sound the above conditions can be written as $\gamma^2 > 1$ and

$$A > 0, B > 1$$

$$\text{for } 0 < c^2 < \min(c_1^2, c_2^2) \text{ with } \alpha < 0.5, \alpha/\beta < 1$$

or

$$A < 0, B < 0 \text{ for } \max(1, c_1^2) < c^2 < \gamma^2 \text{ with } \alpha, \beta > 0.$$

Thus in both cases we have a low-velocity range (the existence depending on α and β) with solutions of type (3.6) and a high-velocity range with solutions of type (3.7). For our numerical simulations in Sec. VI we have chosen physical parameters in such a way that the first condition is fulfilled. Due to the light masses of the protons this is likely to be the case in physical systems. For more details see Sec. VI.

The energy of our solutions can be calculated in both parameter areas by inserting the explicit solutions into the expression for the Hamiltonian density. In fact, this calculation can be done analytically but the resulting expression for the energy is rather lengthy. In Fig. 6 this expression is drawn as a function of the velocity for a special set of parameters (see discussion in Sec. VI). In order to give some insight into the general behavior of the energy as a function of velocity we note here that the general expression has a pole at the sound velocity $c = 1$ (hydrogen sublattice), it is also infinite at the sound velocity

$c = \gamma$ (oxygen sublattice), and has a pole at the intermediate velocity $c = \min(c_1, c_2)$. Of special interest is the energy expression for the static kink. Here one finds (assuming $\alpha < 0.5$, $\alpha/\beta < 1$)

$$E(c=0) = E_0$$

$$= (\beta/\alpha - 1)^{1/2} \left[\left[1 - \frac{1}{8\alpha} \right] \arcsin(2\alpha)^{1/2} + \alpha \left[1 + \frac{1}{4\alpha} \right] \left[\frac{1}{2\alpha} - 1 \right]^{1/2} \right]. \quad (4.4)$$

In the case of vanishing coupling between the oxygen and the hydrogen sublattice this reduces to the energy of a static kink in a monoatomic ϕ^4 chain.

$$E_0 = 4(2\beta)^{1/2}/3. \quad (4.5)$$

For numerical calculation it is necessary to have an estimate of the various parameters. We give here a brief description of the "physical" parameter set used later (set 2 in Table I). From Raman and infrared spectra the oxygen-oxygen stretching frequency Ω_{O-O} and the oxygen-hydrogen frequency Ω_{O-H} can be estimated to be^{10,11} $\Omega_{O-O} \simeq 1.9 \times 10^{13}$ Hz, $\Omega_{O-H} \simeq 4.7 \times 10^{14}$ Hz. The potential barrier in the double minimum potential may be assumed to be of the order of 0.5 eV.¹⁵ In our parameter set 2 (see Table I) we used the Yomosa value for Ω_{O-O} directly to determine Ω_1 . The parameter ϵ in the ϕ^4 potential was taken to be 0.4 eV. The oxygen-hydrogen stretching frequency Ω_{O-H} is given in terms of our model parameters by the optical branch of the dispersion relation [see Eq. (5.2)] as $\Omega_{O-H} = 1.8 \times 10^{14}$ Hz. This is of the order of Yomosa's value. Another check of the parameter set is the energy of the static kink for which we find $E_0 = 2.6$ eV. In terms of the dimensionless parameters γ^2, α, β set 2 is equivalent to $\gamma^2 = 0.0075$; $\alpha = 0.0016$; $\beta = 0.08$. For further details see Sec. VI.

V. LINEARIZED LATTICE

In Sec. VI the stability of the solution (3.6) and (3.7) is considered. In contrast to the work by Laedke *et al.*¹²

TABLE I. Sets of model parameters used in the numerical simulations. This table lists also some physical constants associated with each set. E_0 is the energy of the static analytic solution.

	Set 1	Set 2
m (a.m.u.)	1	1
M (a.m.u.)	16	16
a (Å)	5	5
b (Å)	1	1
ϵ (eV)	2	0.4
ω_1 (t.u. ⁻¹)	6	2.218
Ω_1 (t.u. ⁻¹)	1	0.1921
χ (eV/Å ³)	0.15	0.10
v_O (Å/t.u.)	5	0.960
v_P (Å/t.u.)	30	11.090
E_0 (eV)	15.939	2.604
v_1 (Å/t.u.)	4.999	0.950

we use numerical simulations in order to get an indication of the stability of the solutions. Before we discuss this point, however, we investigate the stability of the lattice in the ground state.

We linearize the equations of motion (2.6) and (2.7) for small fluctuations around the equilibrium position. This is achieved by the ansatz

$$\begin{aligned}\varphi(y, \tau) &= 1 + \epsilon_1 e^{i(qy - \omega\tau)}, \\ \psi(y, \tau) &= \epsilon_2 e^{i(qy - \omega\tau)},\end{aligned}\quad (5.1)$$

where only linear terms in ϵ_1, ϵ_2 are considered. The resulting dispersion relation can be given exactly by

$$\omega_{\pm}^2(q) = F \left[1 \pm \left[1 - \frac{G}{F^2} \right]^{1/2} \right], \quad (5.2)$$

where F and G are functions of the wave number q

$$\begin{aligned}F &= \frac{1}{2} [q^2(1 + \gamma^2) + 8\beta], \\ G &= q^2\gamma^2[q^2 + 8\beta - \alpha(q^2 + 4)].\end{aligned}\quad (5.3)$$

The stability of the lattice is now given by the condition

$$\omega_{\pm}^2(q) \geq 0$$

for all q within the Brillouin zone. In the case of $\gamma^2 < 1$ (only this case is considered later on) a straightforward examination of (5.2) yields the condition for α and β

$$\frac{\alpha}{\beta} \leq \min \left[2, \frac{8}{4 + \pi^2(1 - 1/\alpha)} \right]. \quad (5.4)$$

We notice here that in both examples of Sec. VI this condition is fulfilled.

VI. NUMERICAL INVESTIGATIONS OF THE DYNAMICS OF THE NONLINEAR EXCITATIONS

We have investigated numerically the dynamics of the solutions presented in the previous sections in order to determine their stability. Moreover the simulations have been performed on the discrete lattice and not in the continuum limit so that discreteness effects, which may be important in these systems, have been studied. In order to make the comparison with real systems easier we have worked with physical units, i.e., we have used the equations of motions that are derived directly from the Hamiltonian defined by Eqs. (2.1)–(2.4):

$$\begin{aligned}m \frac{d^2 u_n}{dt^2} &= m \omega_1^2 (u_{n+1} + u_{n-1} - 2u_n) \\ &+ \frac{4\epsilon}{b^2} u_n \left[1 - \frac{u_n^2}{b^2} \right] + 2\chi u_n (q_{n+1} - q_n),\end{aligned}\quad (6.1)$$

$$\begin{aligned}M \frac{d^2 q_n}{dt^2} &= M \Omega_1^2 (q_{n+1} + q_{n-1} - 2q_n) \\ &- \chi (u_n - u_{n-1})(u_n + u_{n-1}).\end{aligned}\quad (6.2)$$

These equations are solved with a fourth-order Runge-Kutta scheme and the time step is chosen small enough

to preserve total energy to an accuracy better than 10^{-3} for the full duration of a simulation. The initial positions and velocities of the proton and oxygen atoms are obtained from the analytical solutions presented in the previous sections. In terms of the physical parameters, the solutions are defined in two velocity domains.

(i) $v > v_O$, where $v_O = a\Omega_1$ is the sound speed in the oxygen sublattice (a is the lattice spacing). This domain corresponds to the case $A < 0, B < 0$ defined previously.

(ii) $0 < v < v_M < v_O$ which corresponds to the case $A > 0, B > 1$, where v_M is a maximum speed in the low-velocity range $v < v_O$ defined by the conditions

$$v_M < v_1 \text{ with } v_1^2 = v_O^2 - \frac{\chi^2 a^2 b^4}{2M\epsilon}, \quad (6.3)$$

which states that the effective barrier in the proton sublattice coupled to the oxygen atoms has to be positive, and

$$v_M < v_2 \text{ with } 2v_2^2 = (v_p^2 + v_O^2) - \left[(v_p^2 - v_O^2)^2 + \frac{4\chi^2 b^2 a^4}{mM} \right]^{1/2},$$

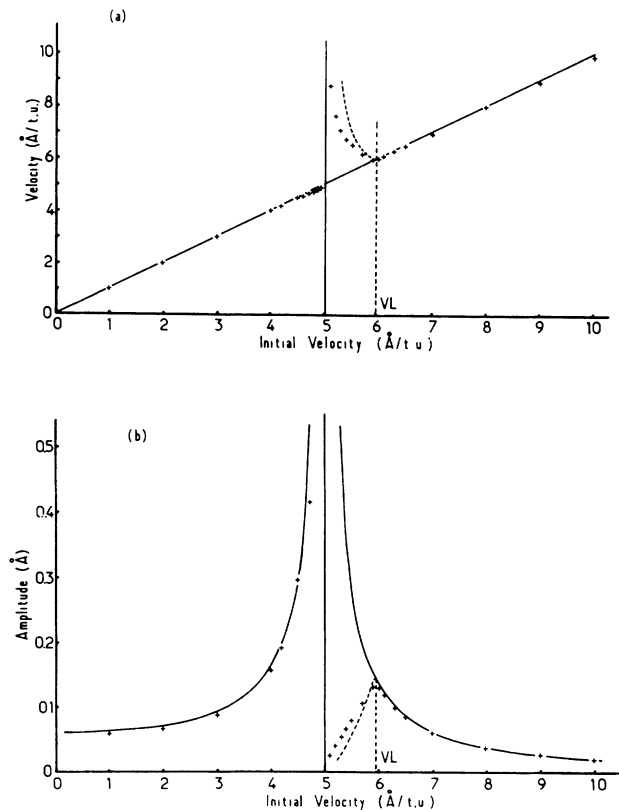


FIG. 2. Velocity (a) and amplitude of the soliton kink (b) vs initial velocity. The solid lines show the values for the analytical solutions; the crosses show the values of the final velocity (a) or amplitude of the oxygen kink (b) when the steady state of the two-component solitary wave has been reached. The dashed line in the range $v > v_O$ indicates the parameters of the high-speed analytical solution which has the same energy as the initial condition (parameter set 1). (t.u. = time unit; see Sec. VI.)

where $v_p = a\omega_1$ is the sound speed in the proton sublattice, which is a condition for the definiteness of the integral used in the calculation of φ . For the parameter sets that we have used in the simulations $v_1 < v_2$. For the protons the implicit solutions (3.6) [case (ii)] or (3.7) [case (i)] written in terms of the physical variables are inverted

numerically and the displacements u_n and velocities \dot{u}_n are simply obtained from the values of the continuum solution for $x = na$

For the oxygen sublattice the analytical solution gives only the derivative $d\psi/dz$ according to Eq. (3.3) and a spatial integration is required to get initial conditions for

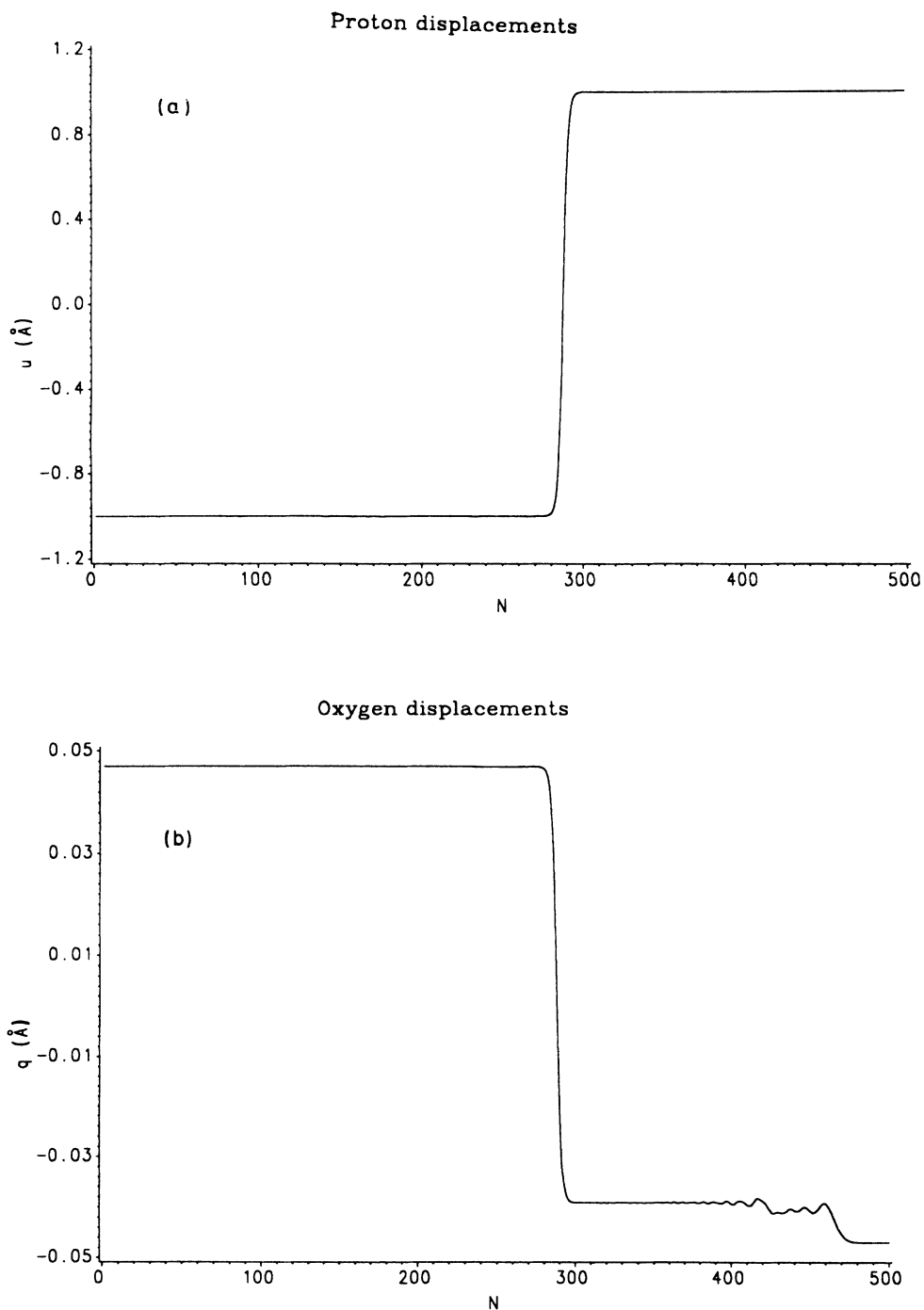


FIG. 3. Proton and oxygen displacements showing the steady-state two-component solitary wave which is generated by an initial condition in the low-velocity range $v < v_1 < v_0$ ($v = 3.0$ Å/t.u. in this case with parameter set 1) where the kink is situated at cell $n = 20$.

the simulations. In order to get the best accuracy for the discrete lattice we have used instead a discrete summation along the finite chain comprising N cells that we simulate, according to

$$q_n = q_1 + \sum_{k=1}^{n-1} f(u_k), \quad n = 2, N \quad (6.4)$$

in which $f(u_k)$ is the expression of $d\psi/dz$ (Eq. 3.3) in terms of the physical parameters. As the model is translationally invariant for the oxygen sublattice, the value of q_1 is not defined. It is chosen in our calculations so that the solution in the oxygen sublattice is centered along the chain in the same cell as the proton kink.

We have defined a system of units which are convenient for the computations: energies are expressed in eV, masses in atomic mass units (a.m.u.), displacements in Å. This defines a time unit (t.u.) equal to 1.0217×10^{-14} s. The simulations have been performed with the two sets of model parameters listed in Table I. Most of the simulations have been performed with set (1) which is identical to the one we used in a previous work¹³ while set (2) has been used to check that the results are preserved in this case which is close to the parameters expected for protons in ice. All simulations have been performed with a chain of 500 cells and the initial kinks were always localized at cell number 20.

A. Stability of the analytical solutions

Figures 2(a) and 2(b) compare the velocity of the two component excitation [Fig. 2(a)] and the amplitude of the

kink in the oxygen sublattice [Fig. 2(b)] in the analytical solution used as the initial condition, and in the final solution which is selected by the system as a function of the velocity v of the initial condition.

In the low-velocity range ($v < v_1$) the initial condition is stable. The analytical solution obtained in the continuum limit provides a good approximation for the two-component solitary wave which propagates as a steady state in the system shown in Fig. 3. However, when v approaches v_1 lattice effects are observed. They are discussed in Sec. VI B.

As shown in Fig. 2, the behavior of the solitary wave in the high-velocity range $v_O < v < v_P$ is more complicated. There exists a velocity domain $v_O < v \leq v_L$ in which the initial condition is unstable. Any initial condition launched in this domain with an initial speed v_i accelerates to the final speed v_F larger than v_L . Simultaneously, the shape of the solitary wave changes and the excitation which emerges after some transient is the same as the solitary wave that is generated by an initial condition almost equal to v_F . Figures 4 and 5 show an example of this behavior. In Fig. 4 the proton soliton velocity versus time is drawn. The acceleration towards the final speed v_F is clearly visible. As shown in Fig. 5, the variation in the amplitude of the oxygen kink between the initial condition at speed v_i and the solution at speed v_F is very large. This causes a large distortion in the oxygen sublattice to be left behind the two-component solitary wave while the kink in the proton sublattice is almost undisturbed by the change in speed. On the contrary, an initial excitation launched with a speed higher than v_L is

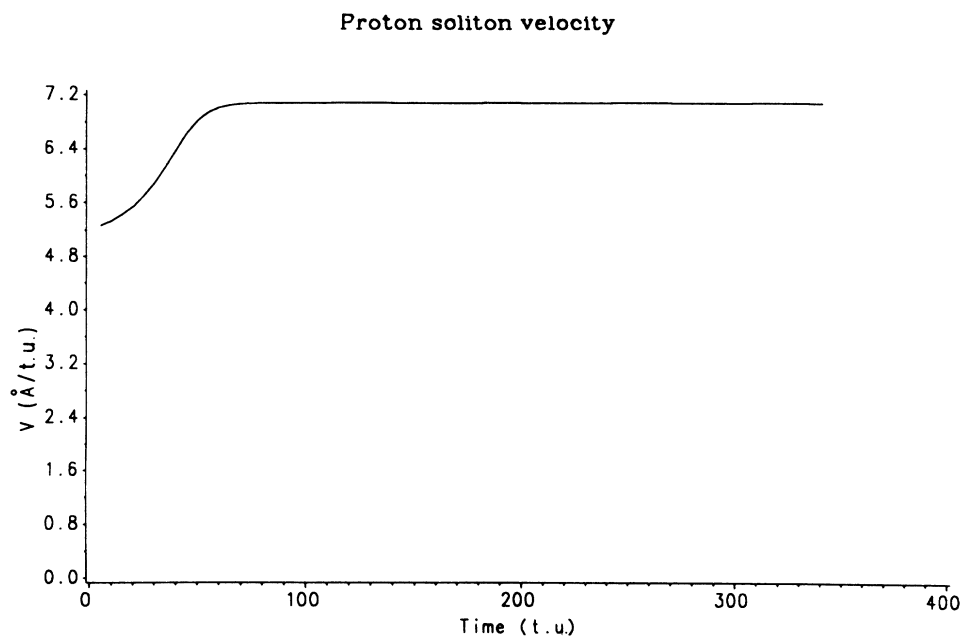


FIG. 4. Velocity vs time of the two-component solitary wave with an initial condition corresponding to a speed $v_O < v < v_L$ ($v = 5.3$ Å/t.u. with parameter set 1).

stable and the final excitation is very close to the initial condition as can be seen in Figs. 2(a) and 2(b).

The origin of the particular velocity v_L which separates a domain in which the initial condition is unstable from a domain in which it is stable can be understood from Fig. 6 in which the energy of the analytical solution is plotted versus its speed v . The speed v_L corresponds to a minimum in the energy and the domain $v_0 < v < v_L$ in which the initial condition is unstable is the only domain

in which the energy decreases as the speed of the solitary wave increases. Due to the U shape of the energy curve in the velocity domain $v > v_0$, a given energy corresponds to two possible solutions in this domain. Initial states $v_0 < v_i < v_L$ lie on the left (unstable) branch of the energy curve and they tend to evolve toward the solution with the same energy on the right (stable) branch with $v_F > v_L$. Although some energy stays in the local deformation of the oxygen sublattice which is left behind the two-

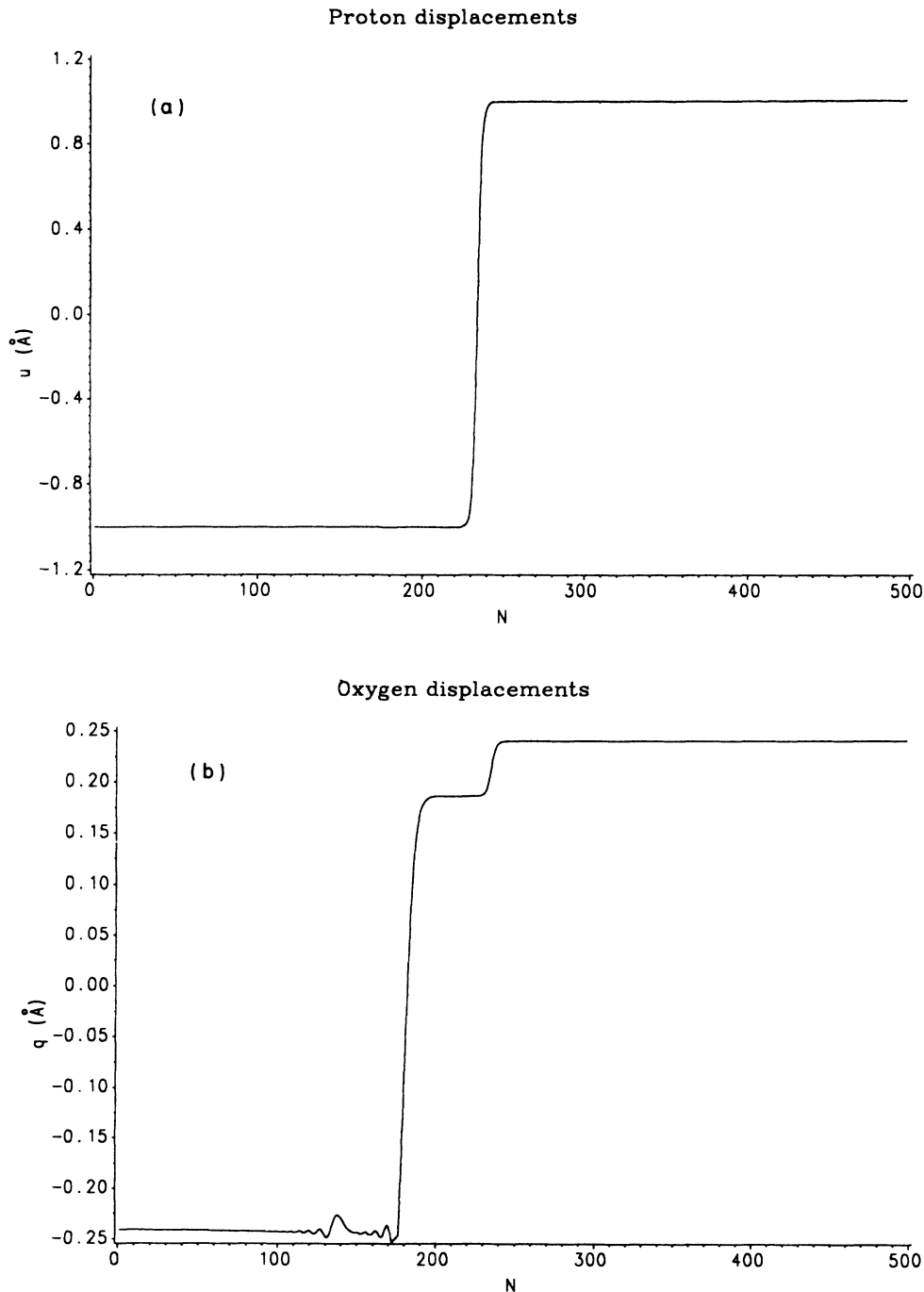


FIG. 5. Proton and oxygen displacements showing the solitary wave and the large distortion in the oxygen sublattice that is left behind (same initial condition as in Fig. 4).

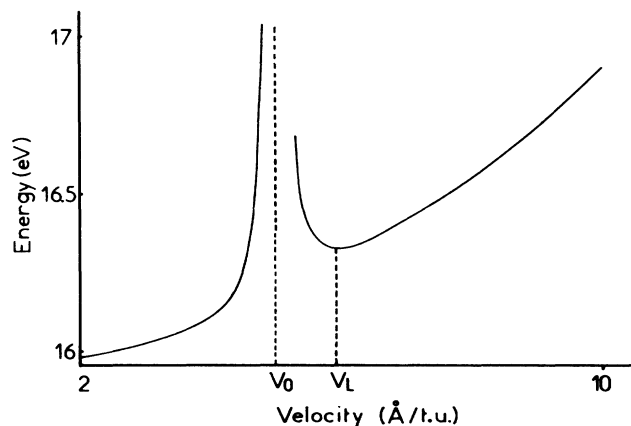


FIG. 6. Energy of the analytic solution vs its speed.

component solitary wave which emerges, this is only a small part of the initial energy so that energy conservation gives a rather good estimate of the final state as shown in Fig. 2 where the dashed lines indicate for each v_i the velocity v_F and amplitude of the analytical solution lying on the right branch of the energy curve.

B. Discreteness effects

As mentioned previously, in the velocity range $0 < v < v_1$ additional features are observed when v approaches v_1 . A typical example is shown in Figs. 7 and 8.

The solitary wave exhibits two noticeable features: (i) the velocity of the proton kink shows regular oscillations around its mean value which is very close to the initial velocity (Fig. 7), and (ii) the kink in the oxygen sublattice radiates a tail of oscillations which is particularly visible on the velocities of the atoms (Fig. 8).

While feature (i) is yet unexplained, the variation of feature (ii) versus the kink velocity indicates clearly that it is created by discreteness effects. The amplitude of the oscillatory tail increases when the solitary-wave velocity approaches v_1 (i.e., becomes very close to the sound speed in the oxygen sublattice) while the frequency of the oscillations decreases. This behavior can be described by a simple theoretical approach that we developed previously for a one-dimensional nonlinear lattice.¹⁶ According to this theory, the oscillatory tail (if any) has a frequency ω and wave vector k , which are determined by the intersection of the dispersion curve of the discrete lattice $\omega^2 = f(k)$ and an "effective dispersion curve" for the solitary wave moving at speed v which is simply $\omega^2 = k^2 v^2$ (Fig. 9). In monatomic lattice, when v is larger than the sound speed (which is the case for solitary waves in nonlinear lattices without competing interactions between second neighbors), the two curves do not intersect (except at the origin) and no radiation is emitted. On the contrary, for a solitary wave moving slower than the sound speed the two curves intersect and radiations are emitted. Moreover, the higher the speed, the larger the radiation. Although the theory was developed for a single chain, the same ideas are valid here if one considers the oxygen sublattice except that the speed of the solitary wave is not determined by the oxygen sublattice but also by the proton sublattice so that both subsonic or supersonic kinks propagate in the oxygens. The case $v < v_1$ corresponds to

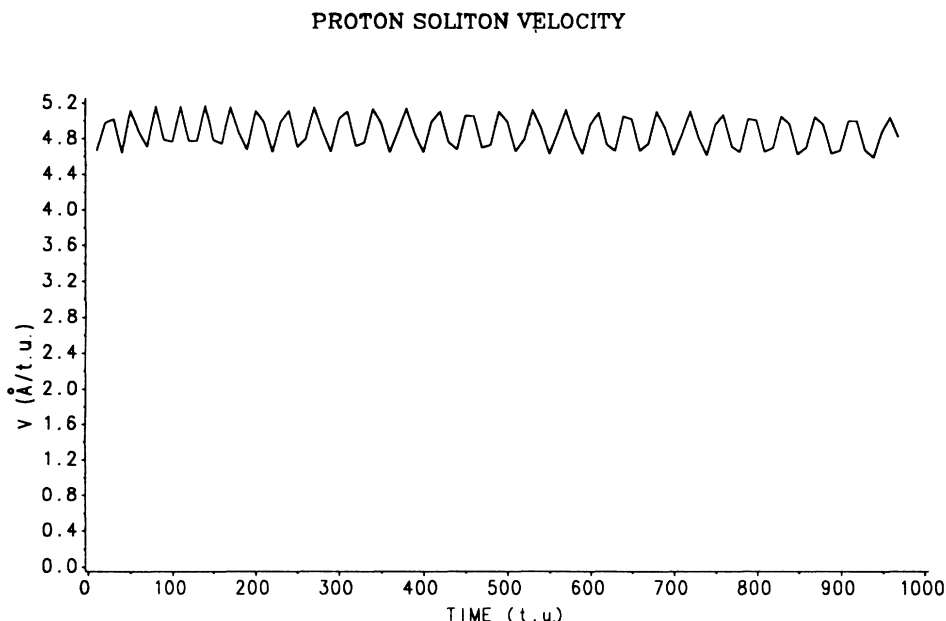


FIG. 7. Variation vs time of the velocity of the proton kink for a solitary wave in the low-velocity domain with a speed close to v_1 .

the subsonic case; thus we expect some radiations to be emitted by the oxygen kink. Moreover, the theory shows that when v increases and approaches the sound speed, the frequency and wavelength of the emitted radiations decrease very fast for small variations in v (see Fig. 9) which is exactly what we observe in the numerical simulations and the quantitative agreement between theory and observation is good. The same analysis explains why

we never find any radiation in the wake of the oxygen kink in the high-velocity range—because its speed is then higher than the sound speed in the oxygen sublattice. It is indeed tempting to also explain the oscillations in the speed of the oscillatory wave by discreteness effects. However, its period is much larger than the time that is required for the solitary wave to move along one cell and we do not yet have an explanation for this phenomenon.

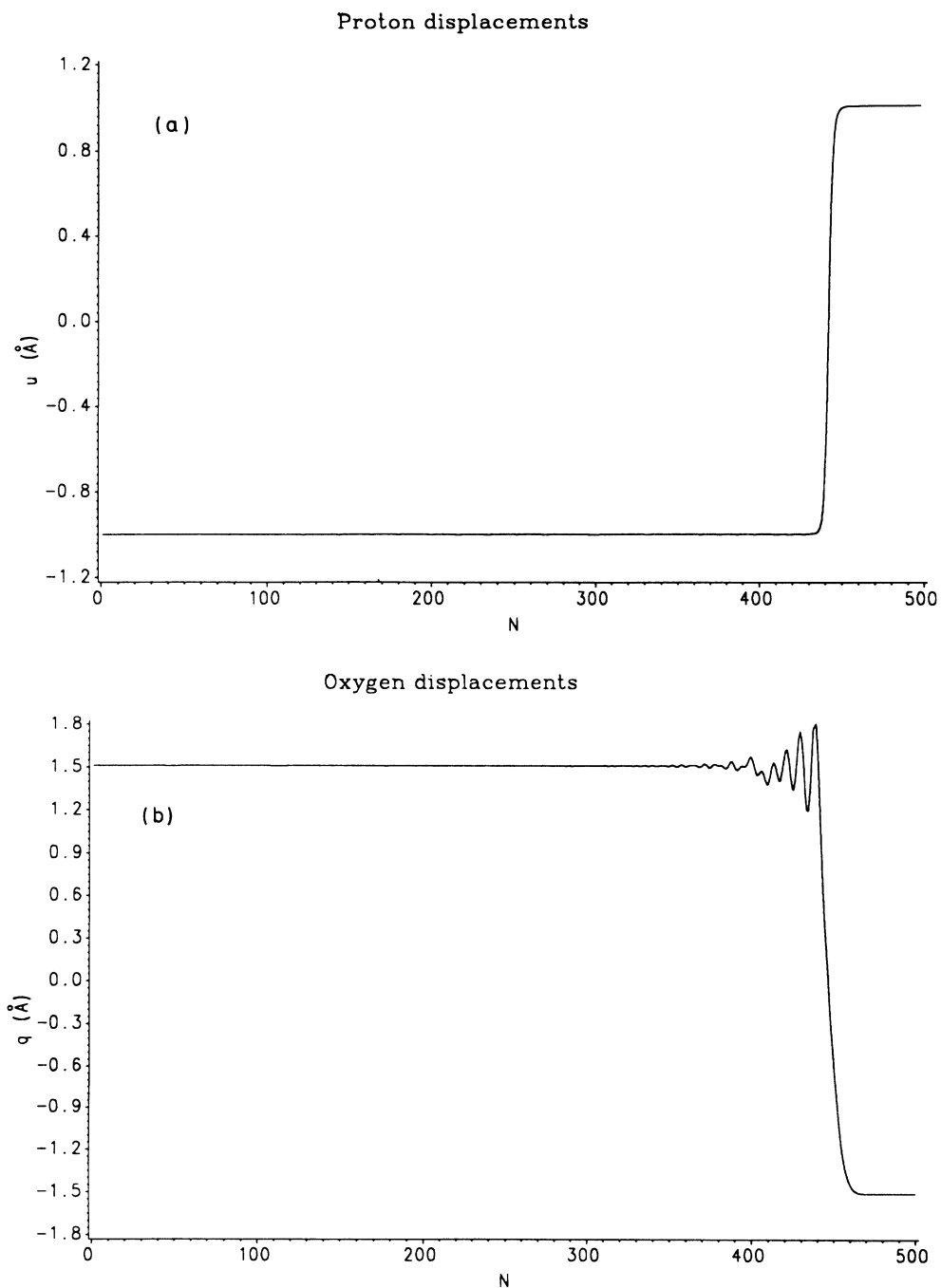


FIG. 8. Displacements of the protons and oxygens at a later time with the same initial conditions as in Fig. 7.

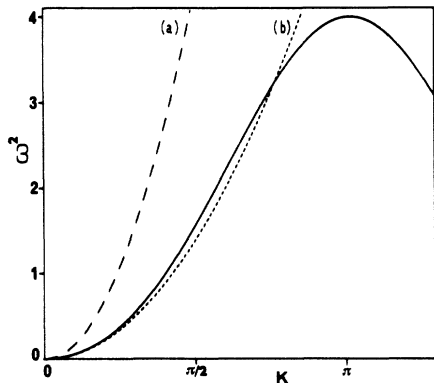


FIG. 9. Dispersion curve of the oxygen sublattice (solid line) and of a kink in the oxygen sublattice moving at velocity $v > v_0$ (a) and $v < v_0$ (b). The wave vector and frequency of the radiation emitted due to discreteness effects are given by the intersection of the two curves.

VII. SUMMARY

We have proposed a model for solitons in hydrogen-bonded chains where the solutions can be given analytically in a wide range of velocities. In addition, a forbid-

den zone was found where no solitary excitations exist. This seems to be a general intrinsic feature of such models not depending on the details of the interaction.¹⁴ Such a forbidden region should perhaps be experimentally detectable in an anomaly in the proton mobility. In order to do the calculations within a realistic model, we have succeeded in establishing a set of parameters which results in physical reasonable values for various energies and frequencies. The stability of the solutions was checked numerically by computer simulations of the discrete model. In the low-velocity region typical discreteness effects exist, while in a small intermediate velocity region (where for a given energy two solutions were possible) a transition to the high-velocity solution was found.

ACKNOWLEDGMENT

One of us (D.H.) acknowledges the full support of the Deutsche Forschungsgemeinschaft through Sonderforschungsbereich 213 (Topomak, Bayreuth).

- ¹V. Ya. Antonchenko, A. S. Davydov, and A. V. Zolotaryuk, *Phys. Status Solidi B* **115**, 631 (1983).
- ²A. V. Zolotaryuk, K. H. Spatschek, and E. W. Laedke, *Phys. Lett.* **101A**, 517 (1984).
- ³J. F. Nagle, M. Mille, and H. J. Morovitz, *J. Chem. Phys.* **72**, 3959 (1980).
- ⁴J. D. Bernal and R. H. Fowler, *J. Chem. Phys.* **1**, 515 (1933).
- ⁵A. S. Davydov, *Phys. Scr.* **20**, 387 (1979).
- ⁶A. R. Bishop, J. A. Krumhansl, and S. E. Trullinger, *Physica* **1D**, 1 (1980).
- ⁷A. S. Davydov, *Solitons in Molecular Systems* (Reidel, Dordrecht, 1985).
- ⁸R. Blinc, *J. Phys. Chem. Sol.* **13**, 204 (1960).

- ⁹P. G. DeGennes, *Solid State Commun.* **1**, 132 (1963).
- ¹⁰S. Yomosa, *J. Phys. Soc. Jpn.* **51**, 3318 (1982).
- ¹¹S. Yomosa, *J. Phys. Soc. Jpn.* **52**, 1866 (1983).
- ¹²E. W. Laedke, K. H. Spatschek, M. Wilkens, Jr., and A. V. Zolotaryuk, *Phys. Rev. A* **32**, 1161 (1985).
- ¹³M. Peyrard, St. Pnevmatikos, and N. Flytzanis, *Phys. Rev. A* **36**, 903 (1987).
- ¹⁴A. V. Zolotaryuk, *Theor. Math. Phys.* **68**, 916 (1986).
- ¹⁵J. Brickmann, *The Hydrogen Bond*, edited by P. Schuster, G. Zundel, and C. Sandorfy (North-Holland, Amsterdam, 1976), p. 217.
- ¹⁶M. Peyrard, St. Pnevmatikos, and N. Flytzanis, *Physica* **19D**, 268 (1986).